January 2007

The vibrational spectra of protonated water clusters: A benchmark for self-consistent-charge density-functional tight binding

Haibo Yu
University of Wollongong, hyu@uow.edu.au

Qiang Cui
University of Wisconsin-Madison

The vibrational spectra of protonated water clusters: A benchmark for self-consistent-charge density-functional tight binding

Abstract

Proton transfers are involved in many chemical processes in solution and in biological systems. Although water molecules have been known to transiently facilitate proton transfers, the possibility that water molecules may serve as the “storage site” for proton in biological systems has only been raised in recent years. To characterize the structural and possibly the dynamic nature of these protonated water clusters, it is important to use effective computational techniques to properly interpret experimental spectroscopic measurements of condensed phase systems. Bearing this goal in mind, we systematically benchmark the self-consistent-charge density-functional tight-binding SCC-DFTB method for the description of vibrational spectra of protonated water clusters in the gas phase, which became available only recently with infrared multiphoton photodissociation and infrared predissociation spectroscopic experiments. It is found that SCC-DFTB qualitatively reproduces the important features in the vibrational spectra of protonated water clusters, especially concerning the characteristic signatures of clusters of various sizes. In agreement with recent ab initio molecular dynamics studies, it is found that dynamical effects play an important role in determining the vibrational properties of these water clusters. Considering computational efficiency, these benchmark calculations suggest that the SCC-DFTB/molecular mechanical approach can be an effective tool for probing the structural and dynamic features of protonated water molecules in biomolecular systems.

Keywords

clusters, water, protonated, charge, spectra, binding, consistent, self, vibrational, benchmark, density, tight, functional, CMMB

Disciplines

Life Sciences | Physical Sciences and Mathematics | Social and Behavioral Sciences

Publication Details

Yu, H. & Cui, Q. (2007). The vibrational spectra of protonated water clusters: A benchmark for self-consistent-charge density-functional tight binding. Journal of Chemical Physics, 127 (23), 234504.

The vibrational spectra of protonated water clusters: A benchmark for self-consistent-charge density-functional tight binding

Haibo Yu[a] and Qiang Cui[b]
Department of Chemistry and Theoretical Chemistry Institute, University of Wisconsin, Madison, Madison, Wisconsin 53706, USA

(Received 19 September 2007; accepted 16 October 2007; published online 19 December 2007)

Proton transfers are involved in many chemical processes in solution and in biological systems. Although water molecules have been known to transiently facilitate proton transfers, the possibility that water molecules may serve as the "storage site" for proton in biological systems has only been raised in recent years. To characterize the structural and possibly the dynamic nature of these protonated water clusters, it is important to use effective computational techniques to properly interpret experimental spectroscopic measurements of condensed phase systems. Bearing this goal in mind, we systematically benchmark the self-consistent-charge density-functional tight-binding (SCC-DFTB) method for the description of vibrational spectra of protonated water clusters in the gas phase, which became available only recently with infrared multiphoton photodissociation and infrared predissociation spectroscopic experiments. It is found that SCC-DFTB qualitatively reproduces the important features in the vibrational spectra of protonated water clusters, especially concerning the characteristic signatures of clusters of various sizes. In agreement with recent *ab initio* molecular dynamics studies, it is found that dynamical effects play an important role in determining the vibrational properties of these water clusters. Considering computational efficiency, these benchmark calculations suggest that the SCC-DFTB/molecular mechanical approach can be an effective tool for probing the structural and dynamic features of protonated water molecules in biomolecular systems. © *2007 American Institute of Physics*. [DOI: 10.1063/1.2806992]

I. INTRODUCTION

Infrared (IR) spectroscopy is a time-honored technique that can provide valuable structural information of various chemical and biological systems with high time resolution.[1,2] The unique value of IR spectroscopy becomes more transparent with the rapid development of various multidimensional techniques in recent years.[3–7] For condensed phase applications, however, the interpretation of IR spectra is not always straightforward, which highlights the importance of developing effective computational techniques that can compute linear and nonlinear IR spectra in complex molecular systems.

An interesting example concerns the application of IR spectroscopy to characterize the protonation state of water clusters in enzyme active sites. Although water molecules are well known to transiently facilitate proton transfers in many different settings, recent Fourier-transform infrared studies found evidence for the existence of long-lived protonated water cluster as the "proton storage site" in bacteriorhodopsin;[8,9] the interpretation seems to be supported by computational studies.[9,10] Recent simulation study of Xu *et al.* also raised a similar possibility in cytochrome c oxidase.[11] To thoroughly examine these proposals, it is imperative to be able to compute reliable IR spectra for water clusters in different protonation states in a biomolecular environment.

As widely recognized, there are at least two different approaches for calculating the IR spectrum.[12] One is based on normal mode analysis (NMA),[13] with either a quantum mechanical (QM),[14] an empirical molecular mechanical (MM),[15] or a QM/MM (Ref. 16) potential function; to consider the effect of thermal fluctuation, it is possible to average the computed IR spectra over a large number of configurations sampled from equilibrium molecular dynamics simulations. Alternatively, a more systematic approach regarding averaging over different conformers and anharmonic motions within the framework of classical mechanics is to compute the IR spectrum by the Fourier transform of the dipole autocorrelation (FT-DAC) function:[17–19]

$$I_{\mathrm{cl}}(\omega) = \frac{1}{2\pi}\int_{-\infty}^{\infty} dt\, \exp[-i\omega t]\langle \boldsymbol{\mu}(0)\cdot\boldsymbol{\mu}(t)\rangle. \tag{1}$$

In this framework, the absorption coefficient is given by

$$\alpha_{\mathrm{QC}}(\omega) = \left[\frac{4\pi^2\omega}{3V\hbar cn(\omega)}\right](1-\exp(-\beta\hbar\omega))Q_{\mathrm{QC}}(\omega)I_{\mathrm{cl}}(\omega), \tag{2}$$

where V is the sample volume, c is the speed of light, and $n(\omega)\simeq 1$ is the refractive index of the medium. Here a quantum correction (Q_{QC}) is included to *approximately* take quantum effects on the nuclear motion into account (see, e.g.,

[a]Electronic mail: haibo@chem.wisc.edu.
[b]Author to whom correspondence should be addressed. Tel.: (+1)-608-262-9801. Fax: (+1)-608-262-4782. Electronic mail: cui@chem.wisc.edu.

Ref. 20 and references therein), which is much less computationally intensive than more rigorous quantum mechanical or semi-classical treatments.[21–23] Various quantum correction factors[23–25] Q_{QC} have been proposed in the literature, and Ramirez *et al.*[20] have shown that the most effective correction for computing the IR intensity of floppy molecules with large anharmonicities is the so-called harmonic correction:

$$Q_{HC} = \frac{\beta\hbar\omega}{1 - \exp[-\beta\hbar\omega]}, \tag{3}$$

which satisfy both detailed balance and the fluctuation-dissipation theorem. With this correction, the theoretical absorption coefficient for the power spectrum is simplified,

$$\alpha_{QC}(\omega) = \left[\frac{4\pi^2\omega}{3V\hbar cn(\omega)}\right]\beta\hbar\omega I_{cl}(\omega). \tag{4}$$

Compared to the NMA based approach, the FT-DAC approach naturally includes the effects of anharmonicity and molecular motion and therefore is more preferable for condensed phase applications. However, to obtain a converged dipole correlation function, extensive molecular dynamics (MD) simulations are required, which puts constraints on the level of QM method in biomolecular applications.

Our plan is to employ the self-consistent-charge density-functional tight-binding (SCC-DFTB) method[26] in a QM/MM framework[27] for interpreting the IR spectra of water clusters in several proton pump systems such as bacteriorhodopsin and cytochrome c oxidase. The computational efficiency of SCC-DFTB makes it, in principle, an attractive choice in this context and complementary to calculations based on much more expensive QM methods that might suffer from convergence issues.[10] Although previous studies based on NMA indicate that SCC-DFTB overall gives favorable vibrational frequencies among semiempirical methods,[28,29] whether it is capable of capturing the spectroscopic signatures of various water clusters remains unknown. In this study, we carry out SCC-DFTB calculations for the IR spectra of various protonated water clusters in the gas phase and compare the results to experimental spectra, which only became available very recently.[30–37] The experimental spectra exhibit different signatures for protonated water clusters of different sizes as well as for their neutral counterparts. Therefore, these characteristic signatures can be used to probe the possible existence and structure of a (protonated/neutral) water network in the active site of enzymes.[8–10]

II. COMPUTATIONAL METHODS

In this section, we outline the technical details for the IR spectrum calculations. In the calculation for each cluster, the entire system is treated quantum mechanically with the original parametrization of the SCC-DFTB approach by Elstner *et al.*. In the NMA based approach, the vibrational analyses are based on the Hessian generated by finite difference of the forces and test calculations show excellent agreement with those based on the analytical Hessian developed by Witek *et al.*[38] The IR intensity for each mode is then calculated by projecting the molecular dipole derivative onto the corresponding eigenvector [see, for example, Eq. (22) in Ref. 16].

For the time correlation based approach, the simulation protocol includes a 5–10 ps constant temperature equilibrium simulation with the Berendsen weak-coupling algorithm with a coupling constant of 0.2 ps (Ref. 39) and a production run, sampling the micro-canonical ensemble, of 100 ps for the small clusters $[H^+(H_2O)_n\ (n=2-10)]$ and 50 ps for the "magic" protonated $H^+(H_2O)_{21}$ cluster. In the experimental studies,[31,34–36] the exact temperatures of the water clusters are either unknown or uncertain. It is estimated that the temperature is in the range of 170 ± 20 K for the magic protonated water clusters.[30,34,40–42] Thus in the current work, we have simulated the cluster $H^+(H_2O)_{21}$ at 100, 125, 150, 175, and 200 K for comparison. To properly sample the high frequency vibrational modes in the system, the time step of integration is set to 0.5 fs, although a shorter time step of 0.2 fs is also tested [see EPAPS (Ref. 43)]. No constraint has been applied to any bond. The coordinates are saved after each step for analysis; in addition, the Mulliken charges are also saved at each step, from which the dipole moment of the system is calculated,

$$\boldsymbol{\mu} = \sum_{i=1}^{n} q_i \mathbf{r}_i, \tag{5}$$

where q_i is the Mulliken charge of atom i and $\mathbf{r}_i$ the coordinates. The infrared spectrum is then calculated with Eqs. (1) and (4) from FT-DAC function using a fast Fourier transform with a Blackman filter to minimize noise.[44] In all the Fourier-transform analysis, 8192 points in the time correlation function are included, which results in a frequency resolution of about 8 cm^{-1} in the power spectrum. For charged systems, the values of the dipole moment as well as its autocorrelation function depend on the choice of the coordinate system. However, since we are interested in the relatively high frequency region (above 1000 cm^{-1}) of the spectrum, the choice of the coordinate system has negligible effects.

In several cases, the Fourier transform of the velocity autocorrelation (FT-VAC) function of the nucleus is also computed. The velocity is recorded every step (at 0.5 fs interval) and no quantum mechanical correction has been applied to the intensities obtained from the Fourier transformation. As pointed out in Ref. 40, FT-DAC is more appropriate for computing IR spectrum due to the natural incorporation of the relevant selection rule, while FT-VAC is expected to be similar to a deep inelastic neutron scattering measurement. In FT-VAC, notable intensity at a certain frequency indicates the existence of a vibrational state, which may involve motions that do not exhibit a change in the dipole moment and hence not being IR active. Nevertheless, FT-VAC generally converges much faster than FT-DAC and FT-VAC is useful for analyzing the motional characters of vibrational modes.

In addition to comparing the calculated spectra to experimental data, the SCC-DFTB results are also compared to B3LYP/6-31+G(d,p) calculations since the latter generally give satisfactory results in previous studies of water clusters.[40,41] First, vibrational spectra based on normal mode analysis at the SCC-DFTB and B3LYP levels are compared for neutral and protonated water dimers. Next, for the

TABLE I. Comparison of the calculated and measured OH stretching vibrational frequencies for the neutral water clusters $(H_2O)_n$, $n=2-5$. The harmonic experimental frequencies are taken from Ref. 57, which were obtained from experimental anharmonic frequencies with the empirically fitted equation $\omega(\text{harmonic}) = 1.0945\omega(\text{anharmonic}) - 168.12\ \text{cm}^{-1}$. All the theoretical values are from harmonic calculations without any anharmonicity corrections. The B3LYP frequencies are obtained with the 6-31+G(d,p) basis set.

ν_{B3LYP} (cm^{-1})	$\nu_{\text{SCC-DFTB}}$ (cm^{-1})	ν_{expt} (cm^{-1})
	$n=2$	
3693	3604	3715
3809	3715	3801
3898	3916	3879
3925	3983	3897
	$n=3$	
3541, 3602, 3616	3511, 3556, 3568	3699
3893, 3898, 3899	3890, 3893, 3899	3910
	$n=4$	
3322, 3428, 3428, 3471	3453, 3514, 3514, 3527	3571
3888, 3889, 3889, 3890	3875, 3880, 3880, 3883	3897
	$n=5$	
3269, 3364, 3379, 3426, 3445	3455, 3493, 3513, 3519, 3533	3509
3887, 3889, 3890, 3892, 3896	3874, 3878, 3880, 3882, 3888	3897

$H^+(H_2O)_2$ and $H^+(H_2O)_4$ clusters, which are reminiscent of the Zundel and Eigen forms of the solvated proton in solution,[45–47] the norm, as well as the components of the dipole moments, is compared at the SCC-DFTB and B3LYP levels; the spectra based on the Fourier transform of the corresponding dipole moment autocorrelation functions are also compared for $H^+(H_2O)_2$.

All SCC-DFTB calculations are carried out with a modified version of CHARMM C32A2.[48] The B3LYP calculations are performed with GAUSSIAN 03.[49]

III. RESULTS

In this section, we first compare SCC-DFTB and B3LYP/6-31+G(d,p) results for normal mode frequencies and dipole moments. Then, we compare the IR spectra calculated at the SCC-DFTB level with experimental data for various small protonated water clusters. Finally, we examine the IR spectrum for a large protonated water cluster with a magic number $(n=21)$ of water molecules. Since the vibrational properties of these clusters have been studied computationally in previous work,[40–42] we only describe the spectral features briefly and focus the discussions mainly on the reliability of the SCC-DFTB results.

A. Normal mode analysis with SCC-DFTB and B3LYP

First the normal mode frequencies at the SCC-DFTB and B3LYP/6-31+G(d,p) levels are compared for both neutral water clusters (Table I) and protonated water clusters (Table II); available experimental data are also shown for comparison. Generally speaking, SCC-DFTB agrees fairly well with B3LYP for the OH stretching vibrational frequencies and those related to the hydrated excess proton; in some cases, however, we note that large differences on the order of $200-400\ \text{cm}^{-1}$ are also present (e.g., H_3O^+ symmetric stretch for protonated water trimer, see Table II). For the neutral water clusters, since the global minima for the clusters from trimer to pentamer are all cyclic, the waters are arranged symmetrically in the clusters leading to a distinction between hydrogen-bonded O–H and free dangling O–H. As the size of the water cluster increases from 2 to 5, the hydrogen-bonded OH stretch becomes lower in frequency while the free dangling OH stretching frequency remains nearly constant at both SCC-DFTB and B3LYP levels, as

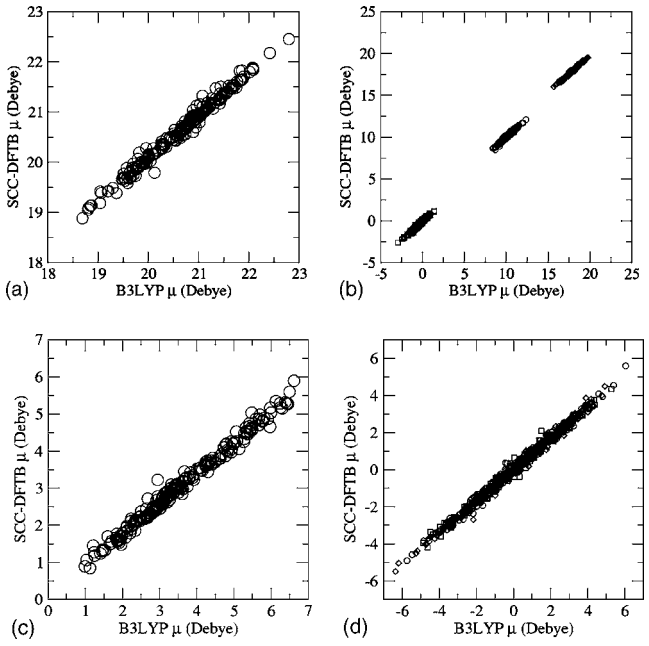

FIG. 1. Comparison of the SCC-DFTB and B3LYP/6-31+G(d,p) dipole moments for 200-water clusters $H^+(H_2O)_2$ and $H^+(H_2O)_4$ sampled from a 100 ps SCC-DFTB simulation at 170 K at 0.5 ps interval. (a) The norm of the dipole moments for the $H^+(H_2O)_2$ clusters. (b) The x,y,z components of the dipole moments for the $H^+(H_2O)_2$ clusters are shown with circle, square, and diamond, respectively. (c) The norm of the dipole moments for the $H^+(H_2O)_4$ clusters. (d) The x,y,z components of the dipole moments for the $H^+(H_2O)_4$ clusters are shown with circle, square, and diamond, respectively.

TABLE II. Comparison of the calculated and measured OH stretching vibrational frequencies for the protonated water clusters $H^+(H_2O)_n$, $n=2-5$. The experimental (fundamental) frequencies and assignments are taken from Ref. 36. All the theoretical values are from harmonic calculations without any anharmonicity corrections. The B3LYP frequencies are obtained with the 6-31+G(d,p) basis set.

Description	ν_{B3LYP} (cm^{-1})	$\nu_{SCC\text{-}DFTB}$ (cm^{-1})	ν_{expt} (cm^{-1})
	$n=2$		
Proton oscillation	1001	1264	1085
H_2O symmetric stretch	3743, 3752	3669, 3678	3520, 3615
H_2O asymmetric stretch	3850, 3851	3913, 3915	3660, 3695
	n=3		
H_3O^+ asymmetric stretch	2389	1982	1880
H_3O^+ symmetric stretch	2554	2377	2420
H_2O symmetric stretch	3793, 3796	3679, 3684	3639
H_3O^+ free OH stretch	3821	3811	3580
H_2O asymmetric stretch	3900, 3903	3934, 3942	3724
	n=4		
H_3O^+ asymmetric stretch	2865, 2867	2768, 2818	2665
H_3O^+ symmetric stretch	2965	2833	
H_2O symmetric stretch	3801, 3802	3685, 3686, 3688	3644
H_2O asymmetric stretch	3907	3944, 3946, 3947	3730
	n=5		
H_3O^+ stretch to AD-type H_2O	2307	1871	1885
H_3O^+ asymmetric stretch	3047	3138	2860
H_3O^+ symmetric stretch	3085	3277	
AD-type H_2O H-bond stretch	3362	3287	3195
H_2O symmetric	3804, 3805, 3807	3688, 3691, 3693	3647
AD-type H_2O free OH stretch	3874	3864	3712
H_2O asymmetric	3911, 3912, 3915	3952, 3955, 3957	3740

measured by experiments. For the protonated water clusters, additionally there are vibrations corresponding to the excess protons, e.g., 1264 cm^{-1} (at the SCC-DFTB level) for the Zundel-like structure in protonated dimer, and 2768, 2818, and 2833 cm^{-1} for the Eigen-like structure in $H^+(H_2O)_4$. However, due to lack of proper sampling over different conformers at the finite temperature in these NMA calculations, a direct comparison with the experimental data is difficult (see below).

B. Dipole moments with SCC-DFTB and B3LYP

Recent work by Otte *et al.*[29] has shown that SCC-DFTB overall reproduces geometric properties very well, so no MD simulations are performed at the B3LYP level. Instead, B3LYP/6-31+G(d,p) single point calculations are carried out for the snapshots harvested during SCC-DFTB molecular dynamics simulations at 170 K. As shown in Fig. 1, both the norm [(a) and (c)] and the x, y, z components [(b) and (d)] of the dipole moments agree well at the SCC-DFTB and B3LYP levels. The correlation coefficients are above 0.99 for the norm of the dipole moments [(a) and (c)] and above 0.98 [(b) and (d)] for their x, y, z components. The error bar for the norm is about 0.14 D for $H^+(H_2O)_2$ and 0.28 D for $H^+(H_2O)_4$.

In Fig. 2, the IR spectra for $H^+(H_2O)_2$ obtained from the dipole autocorrelation function with SCC-DFTB are compared with those with the B3LYP dipole moments. Overall, excellent agreement is found, which is expected given the close agreement in the dipole moments in Fig. 1. The only exception is that SCC-DFTB slightly underestimates the intensity of the OH stretch in the 3500 cm^{-1} region. Considering that the computational cost of B3LYP is about 1000 times that of SCC-DFTB, the agreements shown in Figs. 1 and 2 suggest that SCC-DFTB likely holds a favorable balance between accuracy and efficiency in terms of describing the IR spectra of protonated water clusters.

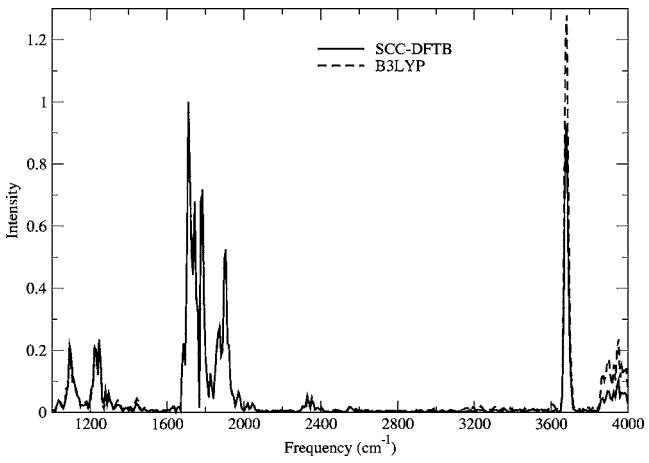

FIG. 2. Comparison between the IR spectra for the protonated water cluster $H^+(H_2O)_2$ from the SCC-DFTB dipole autocorrelation function and the B3LYP dipole autocorrelation function. The B3LYP dipole moment is obtained from single point calculations on the snapshots from the MD simulations with SCC-DFTB.

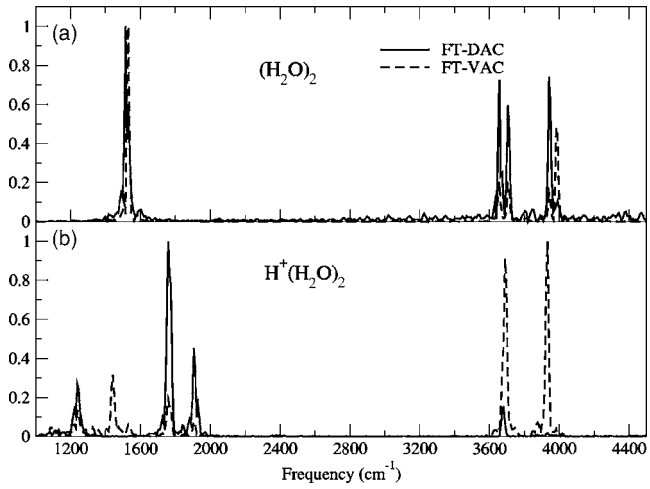

FIG. 3. The IR spectra of the (a) neutral and (b) protonated water dimers at 170 K obtained with the dipole autocorrelation function and the velocity autocorrelation function.

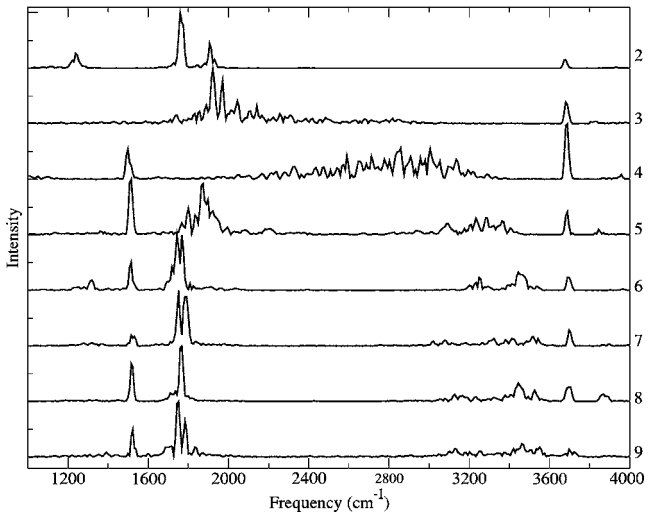

FIG. 4. The IR spectra of the protonated water clusters $H^+(H_2O)_n$ ($n=2-9$) at 170 K. The intensities are normalized to have the maximal intensity in the range of 0–4000 cm^{-1} to be 1.

C. Comparison between water clusters of various sizes

First we compare the IR spectra for the neutral water dimer $(H_2O)_2$ and its protonated counterpart $H^+(H_2O)_2$ at 170 K (Fig. 3). Three distinguished sets of peaks are observed in the neutral water spectrum with both FT-DAC and FT-VAC. They can be easily assigned to the bending mode at $\sim$ 1530 cm^{-1}, the symmetric OH stretching centered at 3600 cm^{-1}, and the asymmetric OH stretching centered at 3910 cm^{-1}, which are consistent with the experimental[50–52] and the previous theoretical[53] spectra. For larger neutral water clusters, the general patterns are very similar to the dimer case (data not shown), which all lack any pronounced spectral signature in the range of 1600–3200 cm^{-1}. By contrast, a rich band of signatures is found in this region for the protonated water dimer [Fig. 3(b)]. The normal mode analysis shows that, at the SCC-DFTB level, the proton oscillation in the Zundel structure of $H^+(H_2O)_2$ is at 1264 cm^{-1} (Table I), which also has a pronounced peak in the computed IR spectra in Fig. 3(b). The peaks around 700–1900 cm^{-1} correspond to the out-of-phase bending vibrations of the flanking water molecules.[37,54,55] For the protonated water clusters, the OH stretching peaks have a lower intensity in the FT-DAC spectrum compared to the FT-VAC spectrum, which has also been observed by Iyengar *et al.*[40,42] The FT-VAC spectra show a peak around 1450 cm^{-1}, which is also present in NMA with a relatively low intensity. The component FT-VAC analyses indicate that this peak is mainly due to the oscillation of the shared proton perpendicular to the O–O axis. However, this band is nearly absent in both the FT-DAC and experimental spectra,[36,37,54,55] indicating that the corresponding mode does not significantly change the dipole moment, i.e., not IR active.

In Fig. 4 the IR spectra of the protonated water clusters $H^+(H_2O)_n$ ($n=2-9$) at 170 K are shown. The three characteristic spectral signatures for the neutral water clusters are also present in many spectra, i.e., the bending mode at $\sim$1500 cm^{-1} and the free OH vibrational stretching at $\sim$3600 and $\sim$3900 cm^{-1}. Consistent with the experimental spectrum of $H^+(H_2O)_4$, a broad peak is present around 2900 cm^{-1}, which matches the symmetric and asymmetric stretchings of the OH in the Eigen-core structure. The average distances between the central O and the three coordinated protons along the trajectory are about 1.02 Å (isotropically fluctuating between 0.94 and 1.17 Å) at 170 K, which is smaller than the value of 1.21 Å (fluctuating between 1.07 and 1.38 Å) in the Zundel-like structure of $H^+(H_2O)_2$. This type of broad spectral signature is persistent in those Eigen-core-like structures (i.e., $\sim$2000 cm^{-1} for $n=3$ and $\sim$1800 cm^{-1} for $n=5$). For $n=6-8$, by contrast, the signatures for the Zundel-like structure of $\sim$1250 cm^{-1}, which correspond to the oscillation of the shared proton in a Zundel ion, are present, most notably for $n=6$ (see Fig. 5). In addition, a pronounced peak in the spectra is seen at $\sim$1750 cm^{-1}, which corresponds to the bending mode in the Zundel ion, as suggested by the experimental study[36] and Car-Parrinello MD (CPMD) simulations.[56]

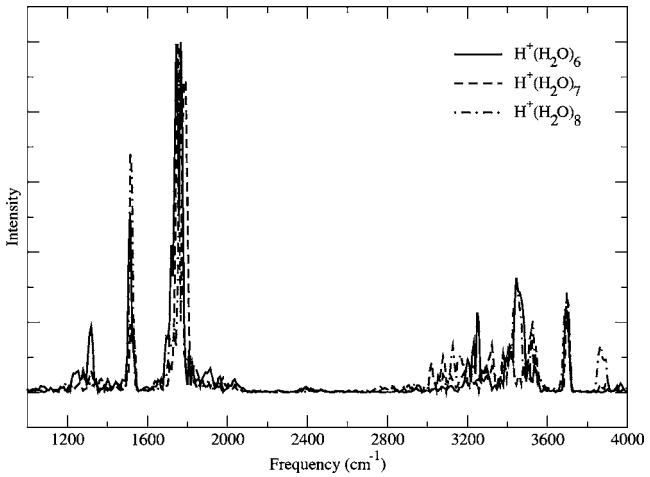

FIG. 5. The IR spectra of the protonated water clusters $H^+(H_2O)_n$ ($n=6-8$) at 170 K. The intensities are normalized to have the maximal intensity in the range of 0–4000 cm^{-1} to be 1.

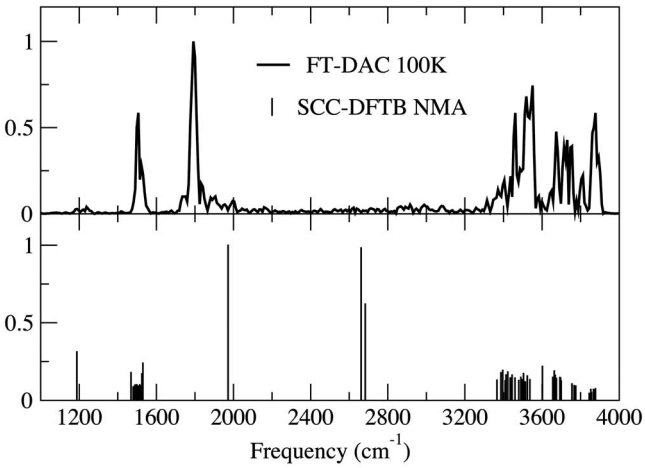

FIG. 6. The IR spectra of $H^+(H_2O)_{21}$ obtained from the dipole autocorrelation function with SCC-DFTB at 100 K and from normal mode analysis.

D. Magic protonated water clusters

Recent theoretical[40–42] and experimental[34,35] studies shed additional insights into the structure, dynamics, and vibrational spectrum of the hydrated proton in the magic 21-water cluster $[H^+(H_2O)_{21}]$, in which the dangling OH stretching modes collapse into a single spectral feature. This also provides a stringent benchmark for the SCC-DFTB approach. In Fig. 6, the IR spectra of protonated 21-water clusters obtained from SCC-DFTB FT-DAC (at 100 K) are compared with SCC-DFTB NMA. Figure 7 shows the IR spectra at five temperatures (100, 125, 150, 175, and 200 K) and of the neutral 21-water cluster at 150 K. Generally the spectra of the protonated 21-water cluster are very similar at the five different temperatures. The most interesting region is around 2000–3000 cm^{-1}, since for smaller protonated water clusters, this region contains spectral signatures for the hydrated excess proton. For the protonated 21-water clusters, however, this region completely lacks any significant intensity the FT-DAC based spectra, consistent with previous theoretical calculations[40–42] as well as the experimental spectra.[34,35] Both current study and previous calculations[40,41] found that significant intensity does appear in this region with normal

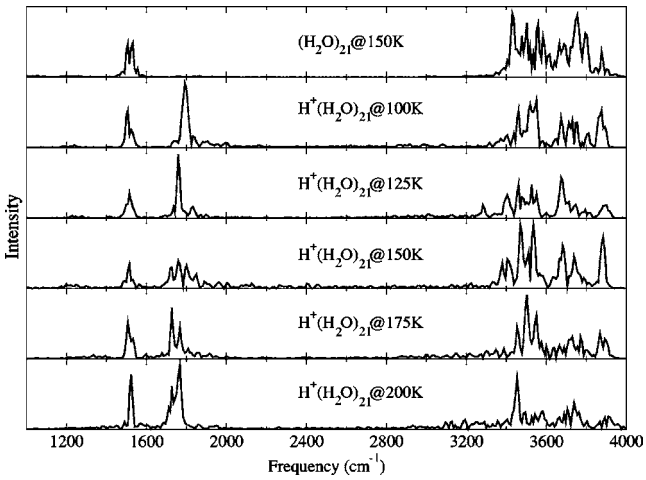

FIG. 7. The IR spectra of $(H_2O)_{21}$ and $H^+(H_2O)_{21}$ obtained by SCC-DFTB simulations at different temperatures.

mode calculations, which is assigned to the OH stretching in $(H_3O)^+$ (Fig. 6). Therefore, the non-negligible dynamical effects at the finite temperature (even as low as 100 K, when the cluster is expected to be solidlike[41]) "average" out the vibrational intensities in this region due to the sampling of multiple structures. Examination of the calculated IR spectra suggests that the peak at ~1750 cm^{-1} corresponds to the excess proton (bending in the Eigen- or Zundel-like structure, in contrast to the water-bending mode at ~1500 cm^{-1}), as seen in the clusters of smaller sizes (Fig. 4). Singh *et al.* have also observed this peak in their Car-Parrinello molecular dynamics simulations, though with a slightly weaker intensity.[41] However, Iyengar[42] has attributed the features at ~1050 and ~1350 cm^{-1}, which are very weak, to the coupled stretch and bending motions of the excess proton. Unfortunately these regions in IR spectrum have not been measured by experiments;[34,35] thus it remains a question whether there are additional signatures besides the features at ~1750 cm^{-1} that correspond to the excess proton.

During the simulation, the excess proton is found to prefer to reside on the surface of the cluster, regardless of the initial structure, which is similar to the previous findings.[35,40,41] Both Eigen and Zundel states are observed under all the temperatures studied here, as in the previous theoretical studies.[40,41] By monitoring the distance between the shared proton and the nearest oxygen atom [Fig. 8(a)], it is found that the percentage of the Zundel form increases as the temperature increases (but not monotonically). This aspect of mixed Eigen-like and Zundel-like states is also seen in Fig. 8(b), in which the radial distribution functions between the most protonated oxygen atom (O^*) and all the other oxygen atoms (O) in the clusters are shown. The inset shows a bimodal distribution between 2.3 and 3.0 Å. The distances between the protonated oxygen atom and the nearest oxygen atoms for $H^+(H_2O)_2$ (Zundel-like) and $H^+(H_2O)_4$ (Eigen-like) optimized with SCC-DFTB are 2.42 and 2.61 Å. Thus this bimodal distribution confirms the presence of both Eigen-like and Zundel-like species in the simulations. A snapshot for each state from the simulation at 100 K is shown in Figs. 8(c) and 8(d), respectively. Compared to previous theoretical studies, the percentile of Zundel-like structures observed in the current study is closer to those observed in Atom-centered Density Matrix Propagation (ADMP) simulations[40] than those in CPMD simulations.[41] Nevertheless, all these studies demonstrate that the sampling of thermally accessible conformations at finite temperatures is crucial for the proper calculation of IR spectra for protonated water clusters, which we expect to hold true in the biomolecular context as well.

IV. CONCLUSIONS

In present work, we have calculated the infrared spectra for various water clusters at the SCC-DFTB level using both normal mode analysis and dipole autocorrelation functions based on classical molecular dynamics simulations. The

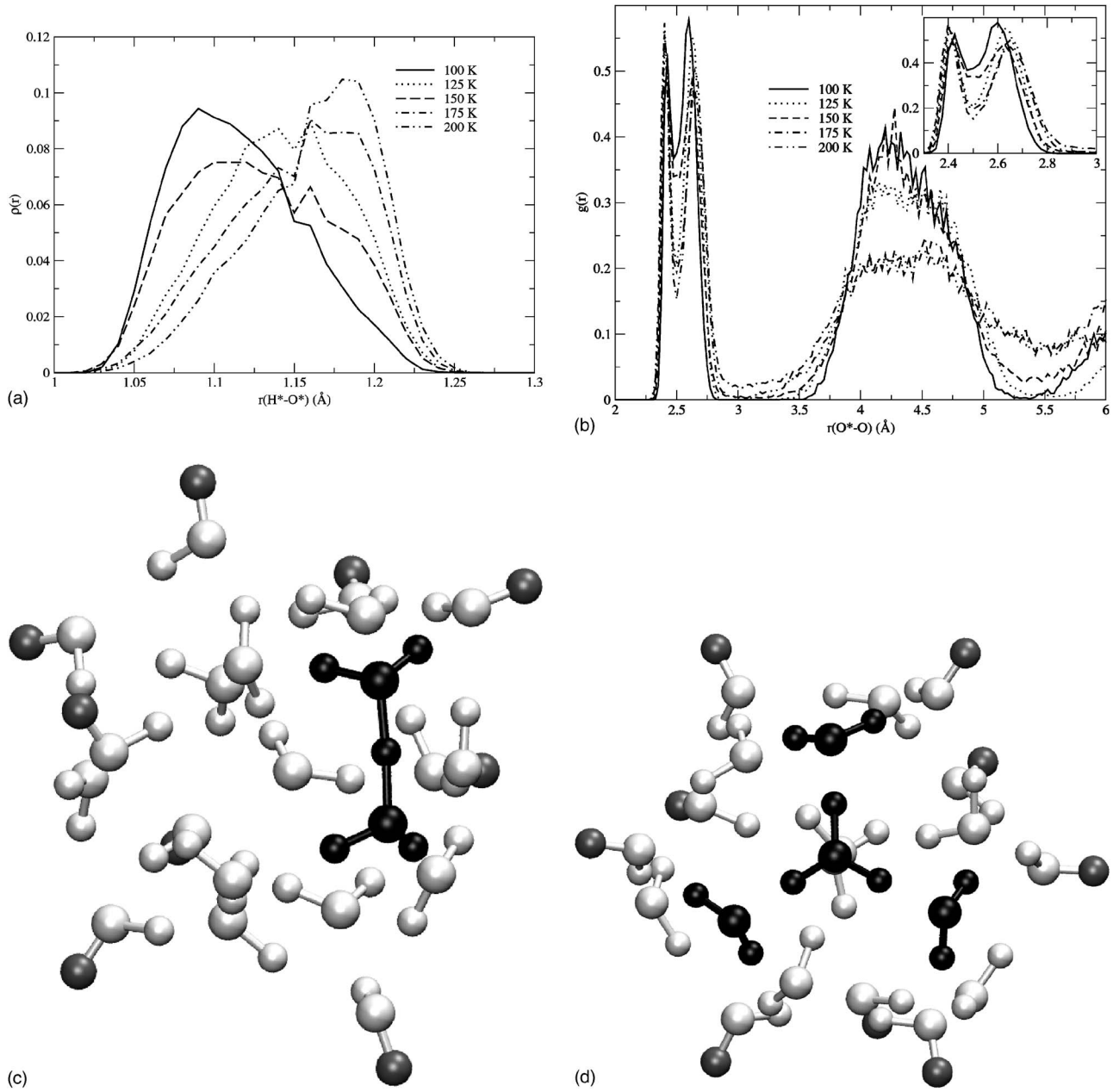

FIG. 8. (a) The distribution of the distance between the excess proton and the nearest oxygen atom in the SCC-DFTB simulations of $H^+(H_2O)_{21}$ at different temperatures. (b) The radial distribution function for the distance between oxygen atom in the protonated water and oxygen atoms in all other water molecules in the cluster at 100 K. The inset shows the signatures of both Zundel and Eigen species. (c) A Zundel ion obtained during MD simulations at 100 K. The protonated species on the surface is highlighted in black and the nine dangling hydrogens are shown in gray. (d) An Eigen ion obtained during MD simulations at 100 K. The protonated species on the surface is highlighted in black and the nine dangling hydrogens are shown in gray.

nuclear quantum effects on the computed IR intensity are approximated using a simple harmonic quantum correction factor, which was found to be effective in previous analysis for floppy molecules with large anharmonicities.[20] By comparing the results with either B3LYP calculations or available experimental data, it is found that SCC-DFTB successfully captures the key features of the vibrational spectra of these systems, especially the difference between neutral and protonated water clusters and spectral signatures of protonated water clusters of different sizes. The high computational efficiency makes SCC-DFTB a potentially appealing method of choice for investigating the spectral properties of biomolecular systems, especially in the framework of QM/MM simulations. In particular, the current work suggests that SCC-DFTB/MM simulations can be applied to effectively probe the protonation state and structure of water clusters in complex biomolecules, although more explicit comparison to experimental data is required to firmly establish this point. Finally, considering the minimal basis nature of SCC-DFTB, it is unlikely that a direct application of the method is suitable for predicting spectra that are sensitive to the polarizability of the system, such as Raman spectra; however, performing conformational sampling with SCC-DFTB and generating the relevant autocorrelation function with single point calculations at the higher level could be a practical strategy for large molecules.

ACKNOWLEDGMENTS

This work is supported by a grant from the National Institutes of Health (R01-GM071428-02). Q.C. is an Alfred P. Sloan Research Fellow. Computational resources from the National Center for Supercomputing Applications at the University of Illinois are greatly appreciated. Discussions with Professor James L. Skinner and Professor Kenneth Jordan are greatly appreciated.

[1] H. H. Mantsch and D. Chapman, *Infrared Spectroscopy of Biomolecules* (Wiley-Liss, New York, 1996).
[2] C. Kotting and K. Gerwert, ChemPhysChem **6**, 881 (2005).
[3] M. T. Zanni and R. M. Hochstrasser, Curr. Opin. Struct. Biol. **11**, 516 (2001).
[4] J. D. Eaves, J. J. Loparo, C. J. Fecko, S. T. Roberts, A. Tokmakoff, and P. L. Geissler, Proc. Natl. Acad. Sci. U.S.A. **102**, 13019 (2005).
[5] C. Kolano, J. Helbing, M. Kozinski, W. Sander, and P. Hamm, Nature (London) **444**, 469 (2006).
[6] I. J. Finkelstein, J. R. Zheng, H. Ishikawa, S. Kim, K. Kwak, and M. D. Fayer, Phys. Chem. Chem. Phys. **9**, 1533 (2007).
[7] R. M. Hochstrasser, Proc. Natl. Acad. Sci. U.S.A. **104**, 14190 (2007).
[8] F. Garczarek, L. S. Brown, J. K. Lanyi, and K. Gerwert, Proc. Natl. Acad. Sci. U.S.A. **102**, 3633 (2005).
[9] F. Garczarek and K. Gerwert, Nature (London) **439**, 109 (2006).
[10] G. Mathias and D. Marx, Proc. Natl. Acad. Sci. U.S.A. **104**, 6980 (2007).
[11] J. C. Xu, M. A. Sharpe, L. Qin, S. Ferguson-Miller, and G. A. Voth, J. Am. Chem. Soc. **129**, 2910 (2007).
[12] M. Schmitz and P. Tavan, *Modern Methods for Theoretical Physical Chemistry of Biopolymers* (Elsevier, Amsterdam, 2006), Chap. 8, pp. 159–176.
[13] E. B. Wilson, J. C. Decius, and P. C. Cross, *Molecular Vibrations* (McGraw-Hill, New York, 1955).
[14] C. Herrmann and M. Reiher, Top. Curr. Chem. **268**, 85 (2007).
[15] P. Derreumaux and G. Vergoten, J. Chem. Phys. **102**, 8586 (1995).
[16] Q. Cui and M. Karplus, J. Chem. Phys. **112**, 1133 (2000).
[17] D. A. McQuarrie, *Statistical Mechanics* (Harper & Row, New York, 1976).
[18] R. G. Gordon, J. Chem. Phys. **43**, 1307 (1965).
[19] R. Kubo, J. Phys. Soc. Jpn. **12**, 570 (1957).
[20] R. Ramirez, T. Lopez-Ciudad, P. Kumar, and D. Marx, J. Chem. Phys. **121**, 3973 (2004).
[21] G. A. Voth, Adv. Chem. Phys. **93**, 135 (1996).
[22] N. Makri, Annu. Rev. Phys. Chem. **50**, 167 (1999).
[23] C. P. Lawrence, A. Nakayama, N. Makri, and J. L. Skinner, J. Chem. Phys. **120**, 6621 (2004).
[24] P. H. Berens, S. R. White, and K. R. Wilson, J. Chem. Phys. **75**, 515 (1981).
[25] J. S. Bader and B. J. Berne, J. Chem. Phys. **100**, 8359 (1994).
[26] M. Elstner, D. Porezag, G. Jungnickel, J. Elsner, M. Haugk, T. Frauenheim, S. Suhai, and G. Seifert, Phys. Rev. B **58**, 7260 (1998).
[27] D. Riccardi, P. Schaefer, Y. Yang, H. B. Yu, N. Ghosh, X. Prat-Resina, P. König, G. H. Li, D. G. Xu, H. Guo *et al.*, J. Phys. Chem. B **110**, 6458 (2006).
[28] H. A. Witek and K. Morokuma, J. Comput. Chem. **25**, 1858 (2004).
[29] N. Otte, M. Scholten, and W. Thiel, J. Phys. Chem. A **111**, 5751 (2007).
[30] J. C. Jiang, Y. S. Wang, H. C. Chang, S. H. Lin, Y. T. Lee, G. Niedner-Schatteburg, and H. C. Chang, J. Am. Chem. Soc. **122**, 1398 (2000).
[31] K. R. Asmis, N. L. Pivonka, G. Santambrogio, M. Brummer, C. Kaposta, D. M. Neumark, and L. Woste, Science **299**, 1375 (2003).
[32] T. D. Fridgen, T. B. McMahon, L. MacAleese, J. Lemaire, and P. Maitre, J. Phys. Chem. A **108**, 9008 (2004).
[33] J. M. Headrick, J. C. Bopp, and M. A. Johnson, J. Chem. Phys. **121**, 11523 (2004).
[34] M. Miyazaki, A. Fujii, T. Ebata, and N. Mikami, Science **304**, 1134 (2004).
[35] J. W. Shin, N. I. Hammer, E. G. Diken, M. A. Johnson, R. S. Walters, T. D. Jaeger, M. A. Duncan, R. A. Christie, and K. D. Jordan, Science **304**, 1137 (2004).
[36] J. M. Headrick, E. G. Diken, R. S. Walters, N. I. Hammer, R. A. Christie, J. Cui, E. M. Myshakin, M. A. Duncan, M. A. Johnson, and K. D. Jordan, Science **308**, 1765 (2005).
[37] N. I. Hammer, E. G. Diken, J. R. Roscioli, M. A. Johnson, E. M. Myshakin, K. D. Jordan, A. B. McCoy, X. Huang, J. M. Bowman, and S. Carter, J. Chem. Phys. **122**, 244301 (2005).
[38] H. A. Witek, S. Irle, and K. Morokuma, J. Chem. Phys. **121**, 5163 (2004).
[39] H. J. C. Berendsen, J. P. M. Postma, W. F. van Gunsteren, A. Di Nola, and J. R. Haak, J. Chem. Phys. **81**, 3684 (1984).
[40] S. S. Iyengar, M. K. Petersen, T. J. F. Day, C. J. Burnham, V. E. Teige, and G. A. Voth, J. Chem. Phys. **123**, 084309 (2005).
[41] N. J. Singh, M. Park, S. K. Min, S. B. Suh, and K. S. Kim, Angew. Chem., Int. Ed. **45**, 3795 (2006).
[42] S. S. Iyengar, J. Chem. Phys. **123**, 216101 (2007).
[43] See EPAPS Document No. E-JCPSA6-127-305745 for the investigation of technical issues that may influence the reliability of the SCC-DFTB results. This document can be reached through a direct link in the online article's HTML reference section or via the EPAPS homepage (http://www.aip.org/pubservs/epaps.html).
[44] M. P. Allen and D. J. Tildesley, *Computer Simulation of Liquids* (Clarendon, Oxford, 1989).
[45] N. Agmon, Chem. Phys. Lett. **244**, 456 (1995).
[46] T. S. Zwier, Science **304**, 1119 (2004).
[47] B. Kirchner, ChemPhysChem **8**, 41 (2007).
[48] B. R. Brooks, R. E. Bruccoleri, B. D. Olafson, D. J. States, S. Swaminathan, and M. Karplus, J. Comput. Chem. **4**, 187 (1983).
[49] M. J. Frisch, G. W. Trucks, H. B. Schlegel, G. E. Scuseria, M. A. Robb, J. R. Cheeseman, J. A. Montgomery, Jr., T. Vreven, K. N. Kudin, J. C. Burant *et al.*, GAUSSIAN 03, Revision C.02, Guassian, Inc., Wallingford, CT, 2004.
[50] M. F. Vernon, D. J. Krajnovich, H. S. Kwok, J. M. Lisy, Y. R. Shen, and Y. T. Lee, J. Chem. Phys. **77**, 47 (1982).
[51] R. H. Page, J. G. Frey, Y. R. Shen, and Y. T. Lee, Chem. Phys. Lett. **106**, 373 (1984).
[52] J. Paul, R. Provencal, C. Chapo, K. Roth, R. Casaes, and R. Saykally, J. Phys. Chem. A **103**, 2972 (1999).
[53] R. A. Wheeler, H. T. Dong, and S. E. Boesch, ChemPhysChem **4**, 382 (2003).
[54] J. Sauer and J. Döbler, ChemPhysChem **6**, 1706 (2005).
[55] O. Vendrell, F. Gatti, and H.-D. Meyer, Angew. Chem., Int. Ed. **46**, 6918 (2007).
[56] I. Shin, M. Park, S. K. Min, E. C. Lee, S. B. Suh, and K. S. Kim, J. Chem. Phys. **125**, 234305 (2006).
[57] J. T. Su, X. Xu, and W. A. Goddard, J. Phys. Chem. A **108**, 10518 (2004).